

## Segmentation of Synthetic Aperture Radar Images by PDE Approach

Maria Mercede Cerimele<sup>1</sup>, Luigi Cinque<sup>2</sup>, Rossella Cossu<sup>1</sup>, Andrea Di Pasquale<sup>3</sup>,  
Roberta Galiffa<sup>2</sup>

<sup>1</sup>*Istituto per le Applicazioni del Calcolo "Mauro Picone", CNR-Roma*  
*m.cerimele@iac.cnr.it*  
*r.cossu@iac.cnr.it*

<sup>2</sup>*Dipartimento Informatica, Sapienza Università di Roma*  
*cinque@di.uniroma1.it*

<sup>3</sup>*Consorzio per l'Informatica e la Telematica, Matera*

### Abstract

In this paper we propose and compare two approaches, based on the level set method in order to extract the coastline from SAR (Synthetic Aperture Radar) images. A coastline is the boundary between land and sea. Detecting the coastline is of fundamental importance when monitoring various natural phenomena such as tides, coastal erosion and the dynamics of glaciers. In this case SAR images show problems which arise from the presence of the speckle noise and of the strong signal deriving from the rough or slight sea. In fact in the case of heavy sea the signal determines an intensity similar to the one of land, making it difficult to distinguish the coastline.

*Keywords:* Level set, SAR image segmentation, anisotropic diffusion

### 1. Introduction

The interpretation of SAR images is an essential component of non-invasive monitoring in many fields such as urban planning, geology (for instance the erosion of coast [1]). In particular, detecting the coastline from SAR (Synthetic Aperture Radar) images is a difficult problem because it is associated with the nature of the signal coming from water and land regions. In fact, the signal return coming from the sea cannot be frequently distinguished from one coming from the land. Moreover, the presence of speckle, modeled as a strong multiplicative noise, makes the coastline detection a very complicated issue.

In this paper we present a level set method applied to the segmentation of SAR images with the aim of extracting two regions (land and sea) from them. This method, proposed by Osher and Sethian [2,3,4] consists in the

identification of an area of interest as the zero level set of an implicit function that evolves according to a PDE (partial differential equation) model with an appropriate speed function. This approach has many advantages: the contours represented by the level set function can split and merge naturally during the evolution and this allows the topological changes to be controlled.

In recent years, active contour methods, based on the evolution of curves and on a *level set* approach [2,3,4] have been an important tool for solving image segmentation problems.

The active contours have been classified as parametric, and are also called *snakes*, or geometrics depending on their representation and implementation. In particular, parametric active contours are explicitly represented as curves parameterized in a Lagrangian reference, whereas the geometric active contours are implicitly represented as two-dimensional functions, called *level sets* that evolve in an Eulerian reference. For SAR images, the parametric active contours were developed in [5,6,7].

In general, in order to extract the contour of a region, the *snake*-model type uses an algorithm that iteratively deforms an initial curve until it reaches the edge of the region to be segmented [2]. However, this model presents several limitations. In fact, since the curve is represented in parametric form, it is discretized by a set of points, so that during the time evolution topological changes are difficult to compute. Moreover, the errors in the representation may be amplified during the numerical computation. Thus, these problems may affect the results of the segmentation process. Compared to the techniques of parametric active contours, the geometric active contours implemented by *level set* have the significant advantage of allowing natural and numerically stable topological changes.

In this paper we use the evolution of curves through *level set* to segment SAR images into two distinct classes, land and sea.

In particular one first approach developed is based on the assumption that each region to segment through *level set* is modeled by a Gamma distribution [8]. In this case an expression of propagation speed of the front is obtained by computing intensity averages of the regions; the method does not need to reduce speckle noise.

A different approach takes into account the problem of filtering speckle noise in the image, which was faced with the application of the SRAD (Speckle Reducing Anisotropic Diffusion) technique [9,10] to SAR image. The paper is organized as follows. In Section 2, the level set method is described. In Section 3, speed computation related to level set method and noise reducing are presented. Some conclusions are drawn in Section 4.

## 2. Mathematical approach

Let  $I: \Omega \rightarrow \mathfrak{R}^n$  be the intensity image function where  $\Omega \subset \mathfrak{R}^2$ .

The goal of image segmentation is to partition  $\Omega$ , moving from image  $I$ , in order to extract disjoint regions covering  $\Omega$ .

The boundaries of these regions may be considered as curves belonging to a family in which time evolution is described by a level set equation. The main advantages of using the level set is that complex shaped regions can be detected and handled implicitly.

In order to obtain the governing equation of a front evolution, we consider a family of parameterized closed contours  $\gamma(x(t), y(t), t) : [0, \infty) \rightarrow \mathfrak{R}^2$ , generated by evolving an initial contour  $\gamma_0(x(0), y(0), 0)$ .

We underline that in the curves evolution theory the geometric shape of the contour is determined by the normal component of the velocity. Supposing that  $\gamma(x(t), y(t), t)$  is a moving front in the image, if we embed this moving front as the zero level of a smooth continuous scalar 3D function  $\phi(x(t), y(t), t)$ , known as the level set function, the implicit contour at any time  $t$  is given by  $\gamma(x(t), y(t), t) \equiv \{(x(t), y(t)) / \phi(x(t), y(t), t) = 0\}$ .

By differentiating with respect to  $t$  the expression  $\phi(x(t), y(t), t) = 0$ , the equation for the evolution of the level set function may be derived

$$(2.1) \quad \frac{\partial \phi(x(t), y(t), t)}{\partial t} + \frac{dx(t)}{dt} \frac{\partial \phi(x(t), y(t), t)}{\partial x} + \frac{dy(t)}{dt} \frac{\partial \phi(x(t), y(t), t)}{\partial y} = 0.$$

We require that the level set function satisfy the condition  $|\nabla \phi(x(t), y(t), t)| \neq 0$  for all  $(x(t), y(t)) \in \gamma(x(t), y(t), t)$ ; this is possible because  $\gamma(x(t), y(t), t)$  is a regular curve. Let  $\mathbf{n} \equiv (n_1, n_2)$  be the unit normal vector to the curve  $\gamma(x(t), y(t), t)$  defined as

$$n_1 = \frac{\frac{\partial \phi(x(t), y(t), t)}{\partial x}}{|\nabla \phi(x(t), y(t), t)|}, \quad n_2 = \frac{\frac{\partial \phi(x(t), y(t), t)}{\partial y}}{|\nabla \phi(x(t), y(t), t)|},$$

that is

$$\begin{aligned} \frac{\partial \phi(x(t), y(t), t)}{\partial x} &= |\nabla \phi(x(t), y(t), t)| n_1, \\ \frac{\partial \phi(x(t), y(t), t)}{\partial y} &= |\nabla \phi(x(t), y(t), t)| n_2. \end{aligned}$$

Substituting in (2.1), we obtain

$$(2.2) \quad \frac{\partial \phi(x(t), y(t), t)}{\partial t} + (n_1 \frac{dx(t)}{dt} + n_2 \frac{dy(t)}{dt}) |\nabla \phi(x(t), y(t), t)| = 0,$$

where  $(n_1 \frac{dx(t)}{dt} + n_2 \frac{dy(t)}{dt})$  describes the curve evolution in the normal direction, so that we can write  $(n_1 \frac{dx(t)}{dt} + n_2 \frac{dy(t)}{dt}) = \frac{d\gamma(x(t), y(t), t)}{dt}$ . Then, (2.2) becomes

$$(2.3) \quad \frac{\partial \phi(x(t), y(t), t)}{\partial t} + \frac{d\gamma(x(t), y(t), t)}{dt} |\nabla \phi(x(t), y(t), t)| = 0,$$

or also

$$(2.4) \quad \frac{d\gamma(x(t), y(t), t)}{dt} = - \frac{\partial \phi(x(t), y(t), t) / \partial t}{|\nabla \phi(x(t), y(t), t)|}.$$

In the following, another important intrinsic geometric property will be used, that is the curvature of each level set, given by

$$(2.5) \quad k(x(t), y(t), t) = -\nabla \cdot \left( \frac{\nabla \phi(x(t), y(t), t)}{|\nabla \phi(x(t), y(t), t)|} \right).$$

We now introduce a function  $v(x(t), y(t), t)$ , named speed function, which is defined as

$$v(x(t), y(t), t) = \frac{d\gamma(x(t), y(t), t)}{dt}.$$

Moreover, for the sake of simplicity, in the following we can write  $\mathbf{x} \equiv (x(t), y(t))$ ,  $\gamma \equiv \gamma(x(t), y(t), t)$  and  $k \equiv k(x(t), y(t), t)$ .

### 2.1. Level Set Implementation

For the numerical approximation of the level set equation in a domain  $\Omega \subset \mathbb{R}^2$  we introduce the computational domain  $\Omega^*$  obtained by considering a uniform partition of  $\Omega$  in  $(N - 1) \times (M - 1)$  disjoint rectangles  $\Omega_{ij}$  with edges  $\Delta x = \Delta y$  which usually in an image are  $\Delta x = \Delta y = 1$ .

Let  $P_{i,j} \equiv P(x_i, y_j)$  ( $i = 1, \dots, N; j = 1, \dots, M$ ) be a point in  $\Omega^*$  and  $\phi_{i,j}^n$  the value of the function  $\phi(\mathbf{x}, t)$  at  $P_{i,j}$  at time  $t^n$ .

The algorithm starts by initializing  $\phi(\mathbf{x}, t)$  as a signed distance function

$$\phi(\mathbf{x}, t = 0) = \pm d$$

where

$$d(\bar{\mathbf{x}}) = \min_{\bar{\mathbf{x}}_\gamma \in \gamma} |\bar{\mathbf{x}} - \bar{\mathbf{x}}_\gamma|.$$

Now, known the value of  $\phi_{i,j}^n$ , the value  $\phi_{i,j}^{n+1}$  is computed by a 2-order ENO scheme with the TVD (Total Variation Diminishing) Runge Kutta scheme for the time integration.

We underline that the definition of  $\phi(\mathbf{x}, t)$  as a signed distance function is crucial. In fact, during the evolution the level set function does not remain

a signed distance function; so that it is necessary to re-initialize the algorithm at regular intervals in order to limit numerical dissipation. Moreover the choice of speed function is a fundamental task for this segmentation approach. This function is computed by the original image, as it is described in the following section.

### 3. Speed Computation and Level Set Segmentation

As mentioned above, the level set method starts from the definition of an initial curve in the domain of the image. In our case, the initial curve on the SAR images is placed in the water zone, so that it surrounds the object of interest (land). The evolution of the initial curve is determined by a speed function, of fundamental choice to achieve a good segmentation. In this paper two different speed functions are introduced and compared. The first uses a speed function based on modeling the intensity of image by a Gamma distribution. The second uses a speed function based on the computation of image gradient.

#### 3.1. Average-based speed

The goal of the segmentation process in this work is to extract two types of regions representing land and sea  $R_i$   $i \in \{1, 2\}$ .

Let  $I(\mathbf{x})$  be the SAR image intensity which we model by a Gamma distribution

$$(3.1) \quad P_{\mu_{R_i}, L}(I(\mathbf{x})) = \frac{L^L}{\mu_{R_i} \Gamma(L)} \left( \frac{I(\mathbf{x})}{\mu_{R_i}} \right)^{L-1} e^{-\frac{LI(\mathbf{x})}{\mu_{R_i}}},$$

where  $L$  is the number of *looks*<sup>a</sup>, that we assume to be the same in the regions and  $\mu_{R_i}$  is the mean intensity given

$$(3.2) \quad \mu_{R_i} = \frac{\int_{R_i} I(\mathbf{x}) d\mathbf{x}}{\int_{R_i} d\mathbf{x}}.$$

Assuming that  $I(\mathbf{x})$  is independent of  $I(\mathbf{y})$  for  $\mathbf{x} \neq \mathbf{y}$ , the segmentation problem consists in finding the regions family  $\hat{R}$  that maximizes the likelihood  $\ell(R|I)$ :

---

<sup>a</sup>The looks are groups of signal samples in a SAR processor that splits the full synthetic aperture into several sub-apertures, each representing an independent look over the identical scene. The resulting image formed by summing these looks is characterized by reduced speckle and degraded spatial resolution.

$$\hat{R} = \arg \max_R \ell(R|I) = \arg \max_R \prod_{i=1}^2 \left( \prod_{\mathbf{x} \in R_i} P_{\mu_{R_i}, L}(I(\mathbf{x})) \right),$$

where  $R = R_i$ . Maximizing  $\ell$  is equivalent to minimizing  $-\log(\ell)$  and then we obtain

$$\hat{R} = \arg \min_R \sum_{i=1}^2 \sum_{\mathbf{x} \in R_i} \left( -\log(P_{\mu_{R_i}, L}(I(\mathbf{x}))) \right).$$

After some algebraic manipulation we obtain

$$(3.3) \quad -\log(\ell(R|I)) = L(a_{R_1} \cdot \log \mu_{R_1} + a_{R_2} \cdot \log \mu_{R_2}) + c(L, I),$$

where  $c(L, I)$  is a constant depending on the image and on the *looks* number, therefore it is independent of the segmentation; while  $a_{R_i}$   $i = 1, 2$  is the area of  $R_i$ :

$$(3.4) \quad a_{R_i} = \int_{R_i} d\mathbf{x}.$$

From (3.3) now the problem is to determine  $\hat{R}$  minimizing the following segmentation criterion:

$$(3.5) \quad F = a_{R_1} \cdot \log \mu_{R_1} + a_{R_2} \cdot \log \mu_{R_2}.$$

We observe that this functional is independent of the *looks* number; moreover the means and the areas depend on the segmentation procedure so that they have to be computed during the segmentation process.

In order to solve the problem of minimizing the previous criterion by a curve evolution in the case of two regions, we consider a plane closed curve  $\gamma(\mathbf{x}, t)$  and we associate its interior region  $R_1$  and its exterior region  $R_2$ :  $R_2 = R_1^c$ , where  $R_1^c$  is the complement to  $R_1$ .

The Euler-Lagrange descent equation corresponding to the functional  $F$  is obtained solving the partial differential equation:

$$(3.6) \quad \frac{d\gamma}{dt} = -\frac{\partial F}{\partial \gamma},$$

where  $\frac{\partial F}{\partial \gamma}$  is the functional derivative of the functional  $F$  with respect to  $\gamma$ . Equating (3.6) and (2.4) we can write

$$(3.7) \quad \frac{\partial \phi(\mathbf{x}, t)}{\partial t} = \frac{\partial F}{\partial \gamma} |\nabla \phi(\mathbf{x}, t)|.$$

Assuming that  $\frac{\partial F}{\partial \gamma} = -v(\mathbf{x}, t)$  ( $\frac{d\gamma}{dt} = v(\mathbf{x}, t)$ ) the level set formulation seeks  $\phi(\mathbf{x}, t)$  s.t.

$$(3.8) \quad \frac{\partial \phi(\mathbf{x}, t)}{\partial t} + v(\mathbf{x}, t)|\nabla \phi(\mathbf{x}, t)| = 0.$$

The segmentation is defined by the convergence for  $t \rightarrow \infty$  of (3.8). In detail we have:

$$(3.9) \quad \frac{\partial F}{\partial \gamma} = \log \mu_{R_1} \frac{\partial a_{R_1}}{\partial \gamma} + \frac{a_{R_1}}{\mu_{R_1}} \frac{\partial \mu_{R_1}}{\partial \gamma} + \log \mu_{R_2} \frac{\partial a_{R_2}}{\partial \gamma} + \frac{a_{R_2}}{\mu_{R_2}} \frac{\partial \mu_{R_2}}{\partial \gamma}.$$

In order to algebraically manipulate the expression (3.8) we recall that if  $f(x)$  is a scalar function, we obtain

$$(3.10) \quad \frac{\partial}{\partial \gamma} \int_{R_\gamma} f(x) dx = f(x) \mathbf{n},$$

where  $\mathbf{n}$  is the external unit normal to the curve  $\gamma$ . Applying the property (3.10) to (3.4) we have

$$(3.11) \quad \frac{\partial a_{R_1}}{\partial \gamma} = \frac{\partial}{\partial \gamma} \int_{R_1} dx = \mathbf{n}.$$

Analogously

$$\frac{\partial a_{R_2}}{\partial \gamma} = -\mathbf{n}.$$

We observe that the minus sign is due to the fact that  $\mathbf{n}$  is the external unit normal to the boundary of  $R_1$ , so the external unit normal to the boundary  $R_2 \equiv R_1^c$ , is  $-\mathbf{n}$ . Now, denoting  $s_{R_i} = \int_{R_i} I(\mathbf{x}) d\mathbf{x} \quad \forall R_i \in R$  and using (3.2) we have:

$$(3.12) \quad \frac{\partial \mu_{R_1}}{\partial \gamma} = \frac{a_{R_1} \frac{\partial s_{R_1}}{\partial \gamma} - s_{R_1} \frac{\partial a_{R_1}}{\partial \gamma}}{a_{R_1}^2}.$$

Applying now (3.10), it holds

$$\frac{\partial s_{R_1}}{\partial \gamma} = \frac{\partial}{\partial \gamma} \int_{R_i} I(\mathbf{x}) d\mathbf{x} = I(\mathbf{x}) \mathbf{n},$$

so that (3.12) becomes

$$(3.13) \quad \frac{\partial \mu_{R_1}}{\partial \gamma} = \frac{a_{R_1} I(\mathbf{x}) \mathbf{n} - s_{R_1} \mathbf{n}}{a_{R_1}^2} = \frac{I(\mathbf{x}) - \mu_{R_1}}{a_{R_1}} \mathbf{n}.$$

Analogously, we have

$$(3.14) \quad \frac{\partial \mu_{R_2}}{\partial \gamma} = -\frac{I(\mathbf{x}) - \mu_{R_2}}{a_{R_2}} \mathbf{n}.$$

Substituting in (3.6) we obtain:

$$(3.15) \quad \frac{\partial F}{\partial \gamma} = \left( \log \mu_{R_1} + \frac{I(\mathbf{x})}{\mu_{R_1}} - \log \mu_{R_2} - \frac{I(\mathbf{x})}{\mu_{R_2}} \right) \mathbf{n}.$$

In some cases, in order to obtain a more regular curve, that is, to remove the small, isolated regions in the final segmentation, it may be necessary to add a regularization term  $-\lambda k \mathbf{n}$  to the previous equation, where  $\lambda \in [0, 1]$  is a positive real constant and  $k$  is the curvature function defined by the expression (2.5). With this regularization term, the final evolution equation for  $\gamma$  is:

$$(3.16) \quad \frac{d\gamma}{dt} = - \left( \log \mu_{R_1} + \frac{I(\mathbf{x})}{\mu_{R_1}} - \log \mu_{R_2} - \frac{I(\mathbf{x})}{\mu_{R_2}} + \lambda k \right) \mathbf{n}.$$

Thus, we obtain the level set equation (3.8), where

$$(3.17) \quad v(\mathbf{x}, t) = \log \frac{\mu_{R_2}}{\mu_{R_1}} + I(\mathbf{x}) \frac{\mu_{R_1} - \mu_{R_2}}{\mu_{R_1} \mu_{R_2}} - \lambda k.$$

At any time during the evolution of the curve the speed values are different, as the two regions change and consequently the means and the areas have to be re-computed.

In Figure 1 we show the segmentation procedure obtained by the average-based speed.

### 3.2. Gradient-based speed

In this subsection the image gradient is used to identify the edges or contours. Indeed, if in a zone the value of the gradient is high then the related pixels correspond to an edge. The gradient-based speed function, in this case, is

$$(3.18) \quad v(\mathbf{x}, t) = -\frac{1}{1 + |\nabla I(\mathbf{x})|^2} - \lambda k.$$

Substituting this expression in (3.8) we obtain the corresponding level set equation.

So, the speed term is defined in such a way that the curve proceeds rather fast in low gradient zones, while it wades through to high gradient ones.

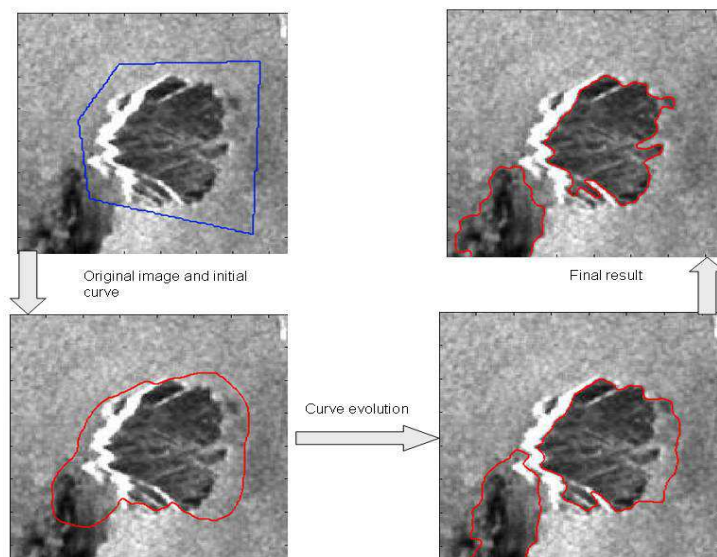


Fig. 1. Average-based speed algorithm

This strategy allows the contour to propagate until it achieves the limits of the coastline in the image and then goes slowly close to those limits.

However, it is well known that in images corrupted by strong noise, the computation of gradient could detect false edges.

Because the SAR images are affected by speckle noise, they are pre-processed by means of the SRAD algorithm (Speckle Reducing Anisotropic Diffusion) which is an extension of Perona-Malik algorithm [9,10]

$$(3.19) \quad \begin{cases} \frac{\partial I(\mathbf{x})}{\partial t} = \nabla \cdot [c(q)\nabla I(\mathbf{x})] \\ I(\mathbf{x}(0)) = I_0 \end{cases}$$

where the diffusion coefficient is

$$(3.20) \quad c(q) = \frac{1}{1 + [q^2(\mathbf{x}) - q_0^2(t)]/[q_0^2(t)(1 + q_0^2(t))]},$$

or

$$(3.21) \quad c(q) = \exp \left\{ -[q^2(\mathbf{x}) - q_0^2(t)]/[q_0^2(t)(1 + q_0^2(t))] \right\},$$

and  $q(\mathbf{x})$  is named instantaneous coefficient of variation and  $q_0(t)$  is the speckle scale function. More precisely

$$(3.22) \quad q^2(\mathbf{x}) = \frac{(1/2)(|\nabla I(\mathbf{x})|/I(\mathbf{x}))^2 - (1/4^2)(\Delta I(\mathbf{x})/I(\mathbf{x}))^2}{[1 + (1/4)(\Delta I(\mathbf{x})/I(\mathbf{x}))^2]},$$

where  $\Delta(\cdot)$  denotes the laplacian operator. The speckle scale function  $q_0(t)$  effectively controls the amount of smoothing applied to the image by SRAD. We observe that in the case of  $N$ -looks SAR image, we can assume  $q_0 = \frac{1}{\sqrt{N}}$ . For the numerical approximation of the equation (3.19) in a computational domain  $\Omega^*$ , let  $I_{i,j}^n$  be the intensity function at the point  $P_{i,j}$  at the time  $t^n$ . The diffusion coefficient  $c(q)$  is calculated according to (3.20) or (3.21) by using the following finite difference approximations for the gradient and the laplacian operators related to the intensity function

$$\begin{aligned}\nabla_R I_{i,j}^n &= [I_{i+1,j}^n - I_{i,j}^n, I_{i,j+1}^n - I_{i,j}^n], \\ \nabla_L I_{i,j}^n &= [I_{i,j}^n - I_{i-1,j}^n, I_{i,j}^n - I_{i,j-1}^n], \\ \Delta I_{i,j}^n &= I_{i+1,j}^n + I_{i-1,j}^n + I_{i,j+1}^n - I_{i,j-1}^n - 4I_{i,j}^n,\end{aligned}$$

with the boundary conditions

$$\begin{aligned}I_{-1,j}^n &= I_{0,j}^n, & I_{m,j}^n &= I_{m-1,j}^n & j &= 0, 1, \dots, n-1, \\ I_{i,-1}^n &= I_{i,0}^n, & I_{i,n}^n &= I_{i,n-1}^n & i &= 0, 1, \dots, m-1.\end{aligned}$$

We recall that in this case  $\Delta x = \Delta y = 1$  and the subscripts  $R$  and  $L$  are the right and the left hand side in the finite difference scheme. Now with the coefficients  $c_{i,j}^n$ , which are the approximation of  $c(q)$  in the domain  $\Omega^*$ , the resulting computational scheme is obtained applying the explicit Euler method to the time integration

$$(3.23) \quad \begin{aligned}I_{i,j}^{n+1} &= I_{i,j}^n + \Delta t [c_{i+1,j}^n (I_{i-1,j}^n - I_{i,j}^n) + c_{i-1,j}^n (I_{i-1,j}^n - I_{i,j}^n) \\ &\quad + c_{i,j-1}^n (I_{i,j-1}^n - I_{i,j}^n) + c_{i,j+1}^n (I_{i,j+1}^n - I_{i,j}^n)].\end{aligned}$$

The intensity function of the image obtained by the convergence of the numerical scheme (3.23) for  $t \rightarrow \infty$ , is now substituted in (3.18) and the resulting expression is used in the level set equation (3.8).

In Figures 2 and 3 we present results obtained applying the SRAD filter and the gradient-based speed, respectively.

#### 4. Conclusions

In this paper we have faced the problem of detecting the coastline from SAR image by the level set method. Two distinct speed evolution functions have been examined. The former, based on the mean intensities of the regions, does not need to reduce speckle noise; the latter, based on the image gradient, takes into account the problem to filter speckle noise by the SRAD technique.

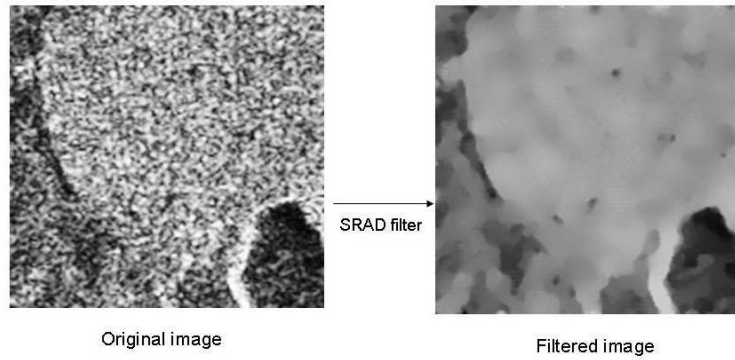


Fig. 2. Result of the anisotropic diffusion filter to reduce speckle noise

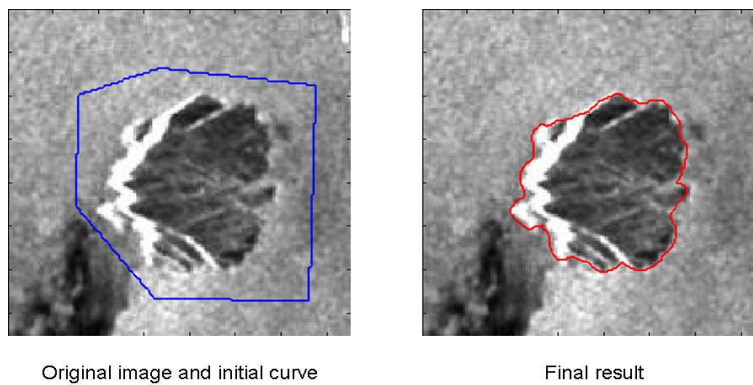


Fig. 3. Final curve (gradient-based speed)

The segmentation obtained by using the first approach detects the coastline with more precision in terms of pixels, since the image is not dealt with filters for noise reduction.

The segmentation obtained by using the speed based on image gradient is less accurate in terms of pixels than the previous one because it works on the filtered image and not on the original one. However, this last approach is independent of the position of the initial curve; whereas the result obtained applying the speed based on mean intensity depends on the position of the initial curve. This problem is due to the fact that the curve is blocked at a local minimum of the segmentation criterion, which does not always coincide with the coastline.

At present we are developing a procedure to combine the positive characteristics of both approaches to improve the segmentation results by the integrated procedure.

This work is part of the research contract with the "Consorzio per l'Informatica e Telematica Innova, Matera", which has provided the PRI (Precision Images) images of ERS Mission.

### Acknowledgements.

The authors wish to thank the anonymous reviewer for his/her comments, which helped to improve the quality of the presentation.

### REFERENCES

1. S. Dellepiane , R. De Laurentiis and F. Giordano, Coastline extraction from SAR images and a method for the evaluation of the coastline precision, *Pattern Recognition Letters* **25** (2004) pp. 1461-147.
2. J. A. Sethian, *Level Set Methods and Fast Marching Methods*, Cambridge University Press, 1999.
3. J. A. Sethian, Evolution, implementation and application of level set and fast marching methods for advancing front, *Journal of Computational Physics*, **169** (2001), pp.503-555.
4. S. Osher and R. Fedkiw. *Level Set Methods and Dynamic Implicit Surfaces*, Springer-Verlag, New York, 2002.
5. M. Kass, A. Witkin, and D. Terzopoulos, Snakes: active contour models, *Journal of Computational Vision*, **1** (1988), pp. 321–333.
6. O. Germain and P. Refregier, Edge location in SAR images: performance of the likelihood ratio filter and accuracy improvement with an active contour approach, *IEEE Trans. Image Processing*, **10** (2001), pp. 72–77.
7. C. Chesnaud, P. Refregier, and V. Boulet, Statistical region snake-based segmentation adapted to different physical noise models, *IEEE Trans. Pattern Analysis and Machine Intelligence*, **21** (1999), pp. 1145–1157.
8. I. Ben Ayed, A. Mitiche, and Z. Belhadj, Multiregion level-set partitioning of synthetic aperture radar images, *IEEE Trans. Pattern Analysis and Machine Intelligence*, **27** (2005), pp. 793–800.
9. Yongjian Yu and Scott T. Acton, Speckle reducing anisotropic diffusion, *IEEE Trans. on Image Processing*, **11** (2002), pp. 1260–1270.
10. P. Perona, J. Malik, Scale space and edge detection using anisotropic diffusion, *IEEE Trans. Pattern Analysis and Machine Intelligence*, **12** (1990), pp. 629–639.